

ERROR COMPENSATION FOR VERY LARGE INFLATABLE REFLECTOR ANTENNAS

William H. Weedon
Applied Radar, Inc.
79 Timberline Road, Warwick, RI 02886
<http://www.appliedradar.com>

Weng Cho Chew and Tie Jun Cui
Electromagnetics Laboratory and
Center for Computational Electromagnetics
University of Illinois, Urbana, IL 61801

Livio Poles
Air Force Research Laboratory AFRL/SNHA
80 Scott Road, Hanscom AFB, MA 01731

Very large inflatable reflector antennas are currently being investigated for medium earth orbit (MEO) space-based radar. The present concept would utilize a reflector antenna with a 60 meter diameter in order to achieve sufficient aperture and power on target from a low-MEO orbit. These large inflatable reflectors are subject to various mechanical errors and shape deformations which would affect the overall performance of the antenna. The mechanical errors could arise from various sources such as seams in the reflector material fabric, holes in the material fabric caused by micrometeors and resulting in uneven pressure distribution, uneven thermal heating, and deformations induced by the platform thrusters. We discuss various approaches to model the effects of these mechanical errors on the overall performance of the reflector antenna. Methods of compensating for the errors using digital beamforming techniques are also discussed.

1. Introduction

Inflatable reflector antennas [1,2] offer an attractive method for achieving a large antenna aperture for high-gain space-based radar and communications applications. One space-based radar application of interest to the Air Force requires a 60 meter diameter reflector antenna in order to achieve sufficient power on target in a low-MEO orbit. The inflatable reflector antenna is attractive because it has a low weight can be easily transported to space on a rocket or space shuttle in a deflated configuration, and inflated once it is orbit.

There are, however, some disadvantages to using an inflatable reflector, rather than a more rigid construction. Firstly, the reflector must be constantly inflated due to holes arising from micrometeors [1] and other punctures and leaks. These leaks often lead to uneven pressure distribution within the reflector, causing surface errors. Uneven thermal heating due to solar radiation is another source of error that may lead to deformation of the reflector surface. Yet another source of surface error arises due to the various acceleration vectors acting at various portions of the structure due to the attached spacecraft thruster activation. The seams in the reflector surface also deform the surface. Figure 1 illustrates a 60 meter reflector and these various sources of error on the reflector surface.

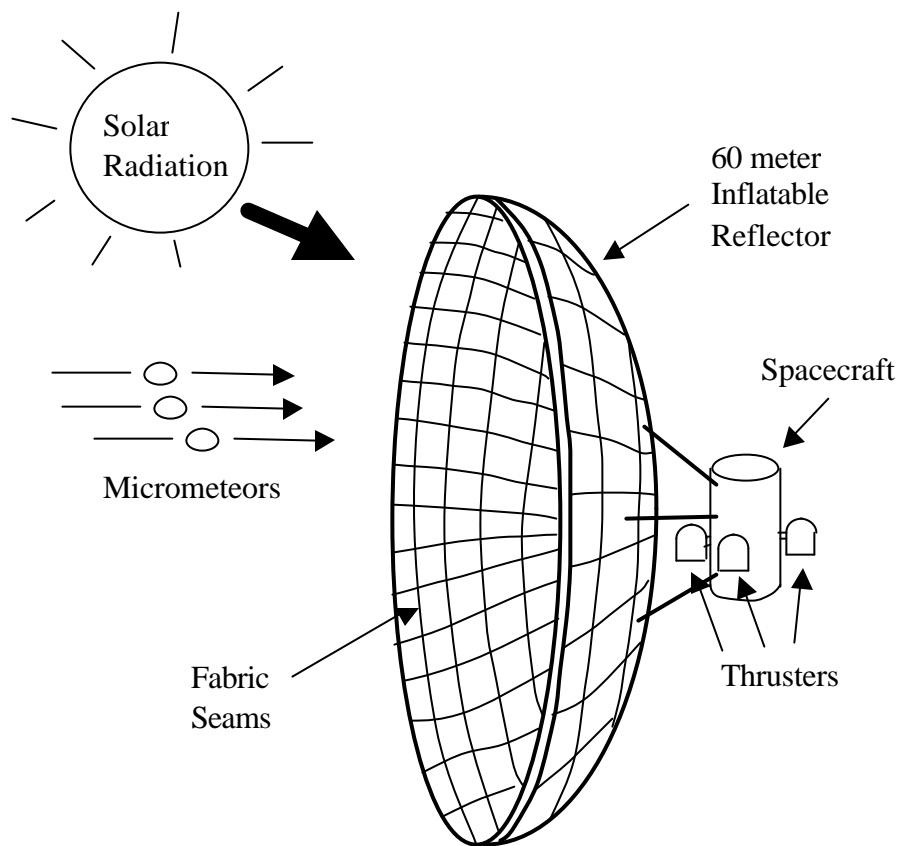


Figure 1: Illustration of a 60 meter inflatable reflector antenna and attached spacecraft showing various sources of reflector surface errors. These errors include spacecraft motion due to activation of spacecraft thrusters, micrometeors which may puncture holes in reflector skin, solar radiation, which induces surface deformations due to uneven thermal heating, and seams in the reflector fabric.

We are concerned here with the effect that these various sources of mechanical error on the reflector surface will have on the overall antenna performance. Depending on the severity of the deformations, the surface errors will have detrimental effects on the antenna main beam and sidelobes. The first stage of our work, therefore, is to model the reflector with the induced surface errors and to get an idea of the antenna performance under various perturbations in the surface.

Assuming that the mechanical surface errors significantly degrade the performance of the antenna, the next question that we wish to address is whether these surface errors can be compensated for using a phased-array feed with transverse equalization. Digital beamforming (DBF) is gaining popularity as a method of forming a phased-array feed, and would be ideally suited for implementing such a transverse equalization procedure. In a practical implementation, the reflector surface errors could be measured in real-time using a raster-scanned laser interferometer located near the feed and used as an input to generate the DBF correction weights.

2. Modeling the Reflector Surface Errors

Independent of the origin of the reflector surface error, whether it be due to thermal effects, leakage or thruster activation, we can model surface errors mathematically as consisting of a “desired” surface, such as a parabolic reflector shape, plus a surface perturbation due to the mechanical errors. The surface perturbations may be modeled as either “continuous” or “segmented”. In the continuous case, the surface errors may be modeled mathematically using either a polynomial or superposition of sinusoids. In the segmented case, the panel seams are considered, which may not be modeled using smooth mathematical functions.

We are currently developing a CAD tool which will generate the geometry required to model surface errors in both the continuous and segmented case. This CAD tool will allow the antenna designer or systems engineer to input the antenna geometry and specify various types and magnitudes of mechanical surface errors. The software will then automatically generate an electromagnetic-compatible mesh in order to compute the antenna gain and radiation pattern using a computational electromagnetic field solver.

3. Radiation Pattern Calculations

There are two general methods for evaluating the radiation pattern of a reflector antenna: aperture-field method and current-distribution method. In the first method, one obtains the far field from the field distribution in the aperture plane,

where it assumes that the reflection from the surface forms a planar wavefront. This is true for a paraboloidal reflector fed at its focus point, but otherwise it is not true. The current-distribution method, however, calculates the far field from the currents induced on the reflector surface because of the primary feed of the feed. Therefore, it is a general method and adopted in shaped antennas.

An easy way to obtain the induced current distribution on the reflector is using the physical optics (PO) approximation [3], which gives

$$\mathbf{J} = 2 \mathbf{n} \times \mathbf{H} \quad (1)$$

where \mathbf{H} is the magnetic field produced by the feed, and \mathbf{n} is the normal direction of the surface. From the induced current \mathbf{J} , one easily obtains the far field pattern.

However, it is not accurate to evaluate the current distribution using the PO method. An exact way to obtain \mathbf{J} is solving an electric field integral equation, which numerically leads to a matrix equation. When the electrical size of the reflector is large, it is impossible to solve the matrix equation by using the conventional LU decomposition method, in which the total CPU time is proportional to N^3 and the storage requirement is of order of $O(N^2)$. To solve the large problem accurately, we use the multilevel fast multipole algorithm (MLFMA) [4,5], in which both the CPU time and storage requirement are only of order of $O(N \log N)$. In the examples we provide, we use 6-level MLFMA.

4. Results

We have computed the radiation patterns for a 60 meter parabolic reflector antenna using both the PO and MLFMA technique. Due to present computer resources on our DEC Alpha computer workstation, we have only computed the patterns at 100 MHz to date. At this frequency, the reflector is 20 wavelengths, and the MLFMA computes the patterns using a full 3-D computational EM code. We plan to extend this solution to 1 GHz and above using an SGI Origin 2000 computer. However, at 1 GHz the reflector is 200 wavelengths in diameter, which is near the maximum problem size that may be solved using the MLFMA with present-day computer resources.

The antenna geometry and electromagnetic mesh are currently generated using the IDEAS software package. Although this software does not allow us to specify arbitrary antenna surface errors as discussed previously, we can generate a

circularly symmetric reflector with circularly symmetric surface perturbations. The geometry is generated as

$$z = \begin{cases} x^2/4f, & \text{for } x \in [0,10) \\ x^2/4f + \epsilon \sin[0.1\pi(x-10)], & \text{for } x \in [10,20) \\ x^2/4f, & \text{for } x \in [20,30]. \end{cases} \quad (2)$$

where z is the reflector normal, f is the focal length of 20 meters, and x is also in meters. This 2-D geometry is then rotated about the z -axis using IDEAS to generate the 3-D circularly symmetric reflector surface.

Figure 2 shows the radiation pattern for a 60 meter reflector antenna computed at 100 MHz using both the PO and MLFMA algorithms. The input source is a horizontal electric dipole placed at the focus. Clearly, the PO algorithm does not adequately model the radiation pattern. The sidelobe computation is particularly poor, although there is also some error in the computation of the mainlobe beamwidth. Figure 3 shows a comparison of the radiation pattern computed using MLFMA with no surface error ($\epsilon = 0$) and with a surface error of ($\epsilon = 0.1$). Figure 4 shows a similar comparison with ($\epsilon = 0.2$).

5. Conclusions

We discussed the modeling of reflector surface errors on a very large diameter inflatable reflector antenna. Radiation patterns were computed using both the PO and MLFMA techniques. The PO method clearly does not model the antenna sidelobes accurately, which justifies the use of the full-wave MLFMA solution. It is expected that reflector surface errors will manifest themselves primarily in the radiation pattern sidelobes. Therefore, it is imperative that the field solver compute the sidelobes accurately. Unfortunately, the modeling of such a large reflector antenna (200 wavelengths at L-band) is pushing the limits of present-day computer resources and computational EM algorithms. Future work will involve not only the modeling of these reflector antenna surface errors, but schemes to correct for these errors using digital beamforming. We also plan to model more general reflector surface errors.

Acknowledgement:

This work is supported by the US Air Force Research Laboratory AFRL/SNHA, Hanscom AFB, MA under contract number F19628-00-C-0058.

References

- [1] C. G. Cassapakis, A. W. Love and A. L. Palisoc, "Inflatable space antennas: a brief overview," Proc. 1998 IEEE Aerospace Conference, Snowmass, CO, March 21-28, 1998.
- [2] M. Thomas, "Inflatable space structures," IEEE Potentials Magazine, pp. 29-32, Dec. 1992.
- [3] C. A. Balanis, Antenna Theory: Analysis and Design, Second Ed., Wiley, NY 1997.
- [4] J. M. Song and W. C. Chew, "Multilevel fast-multipole algorithm for solving combined field integral equations of electromagnetic scattering," Micro. Opt. Tech. Lett., vol. 10, no. 1, pp. 14-19, Sept. 1995.
- [5] J. M. Song, C. C. Lu and W. C. Chew, "MLFMA for electromagnetic scattering from large complex objects," IEEE Trans. Antennas Propagat., vol. 45, no. 10, pp. 1488-1493, Oct. 1997.

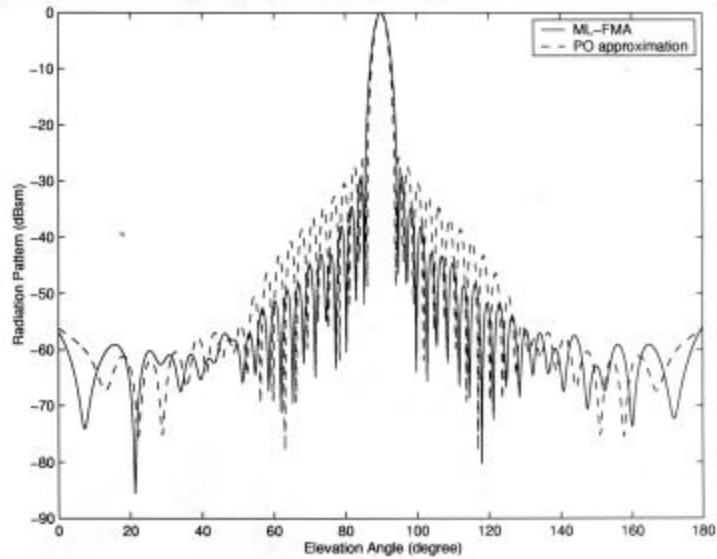


Figure 2: Comparison of PO and MLFMA solutions for a 60 meter parabolic reflector antenna at 100 MHz (200 wavelength diameter) with no surface errors. The PO solution does not accurately model the sidelobes.

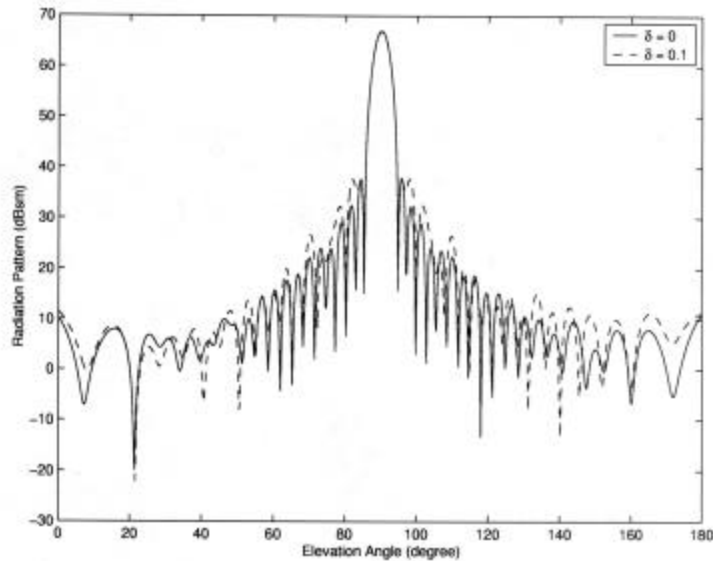


Figure 3: Comparison of 60 meter inflatable reflector with no errors ($\delta = 0$) and reflector with errors ($\delta = 0.1$) in Equation (2). Both solutions computed using MLFMA.

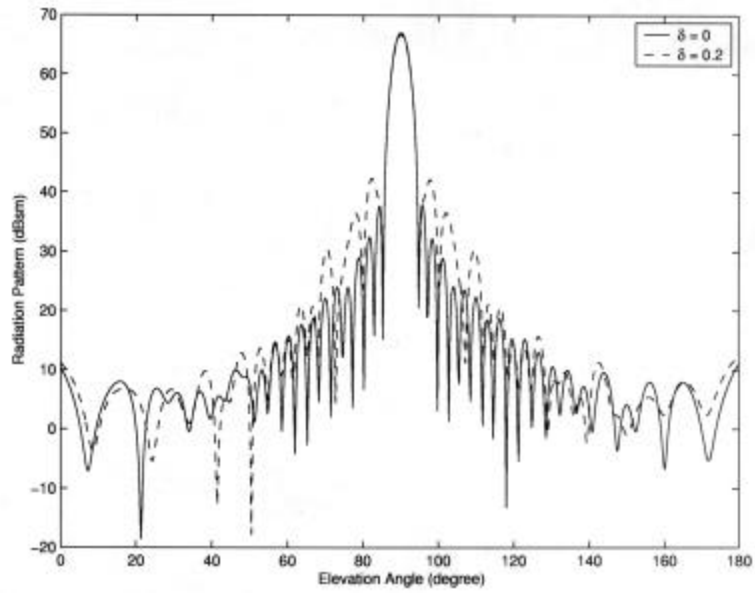


Figure 4: Comparison of 60 meter inflatable reflector with no errors ($\delta = 0$) and reflector with errors ($\delta = 0.2$) in Equation (2). Both solutions computed using MLFMA.